DOPPLER-BRIGHTENING EFFECT IN ROTATING AND EXPANDING OPTICALLY THIN FILAMENTS

B. ROMPOLT and T. ÇIURLA

Astronomical Observatory of the Wrocław University, Wrocław, Poland

Abstract. Profiles of the H_α-line, produced by an optically thin and Doppler brightened filament were computed. The main mechanism of the line broadening was assumed to be either the rotation with a simultaneous radial escape of the filament from the Sun, or the expansion of the filament. The filaments, structured as full cylinders or cylindrical shells of various sizes, were adopted. The computation yielded profiles of essentially different shape, depending on the velocity distribution. The profiles produced by a rotating and escaping filament, viewed against the disk, exhibit asymmetry not only in the wavelength extension of both the wings, but also in the maximum intensity of both the peaks. Some of the profiles are similar in general shape to the profiles of moustaches, surges and loops.

1. Introduction

This paper is the continuation of the investigations, reported by one of us during the present Meeting (Rompolt, 1974b — further quoted as Paper I). Now, we would like to show the other possible mechanisms leading to the modification of the profiles of lines by the Doppler-brightening effect, acting in rotating, as well as in expanding, optically thin filaments. Assumptions and denotations introduced in Paper I are also valid throughout this paper.

2. The Rotation and the Escape

It is known that some fine filamentary, arched or loop-like structures evolve in the solar atmosphere, so that they are in a state of motion with respect to the Sun's surface. For example, some loops expand as a whole, so that their top parts escape (recede) from the Sun. On very rare occasions the loops collapse; at that time their top parts fall down to the solar surface. The top part of the arches or loops, considered here, will be approximated for the purpose of this paper by a filament of cylindrical symmetry.

The existence of rotational or tightly wound spiral mass motions in some fine solar structures was documented by a number of authors (see the review paper Rompolt, 1971; and also Rompolt, 1974a). It is possible that a fine filament, being in a rotational motion at the same time, recedes from the Sun's surface. If this is so, the magnitude of the Doppler brightening at every point of the filament will depend upon the velocity, which is a sum of the velocity of rotation and the velocity of escape.

The way in which the Doppler-brightened lines due to the rotating and escaping filaments are formed is schematically illustrated in Figure 1. A horizontally oriented rotating filament is placed at some height above the photosphere. The filament, assumed to be optically thin, scatters a small portion from the incident Sun's radiation in all directions. The assumed Gaussian profile of the radiation, scattered by every elementary volume of the filament, is Doppler-brightened according to the magnitude and direction of the resultant velocity. Moreover, every elementary profile is to be placed at the proper wavelength position according to the value of the line-of-sight velocity component of its elementary volume. The vectors in Figure 1 are: the thin vector denotes the velocity of rotation, the thick vector indicates the velocity of escape, the broken vector defines the magnitude of the Doppler brightening, and the contour vector is the line-of sight velocity component, taken along one of the two considered directions to the observer.

The profile due to the filament, seen above the limb (the limb profile), is symmetric, while the profile due to the filament, seen against the disk (the disk profile), is asymmetric. The asymmetry of a disk profile manifests itself not only in the

wavelength extension of both the wings, but also in the maximum intensity of both the peaks. It is interesting to note that in the considered case the unequal volumes of a rotating filament participate in the formation of the blue and the red parts of the line. The broken line, vertically oriented to the Sun in Figure 1, is the boundary dividing these two volumes of unequal size.

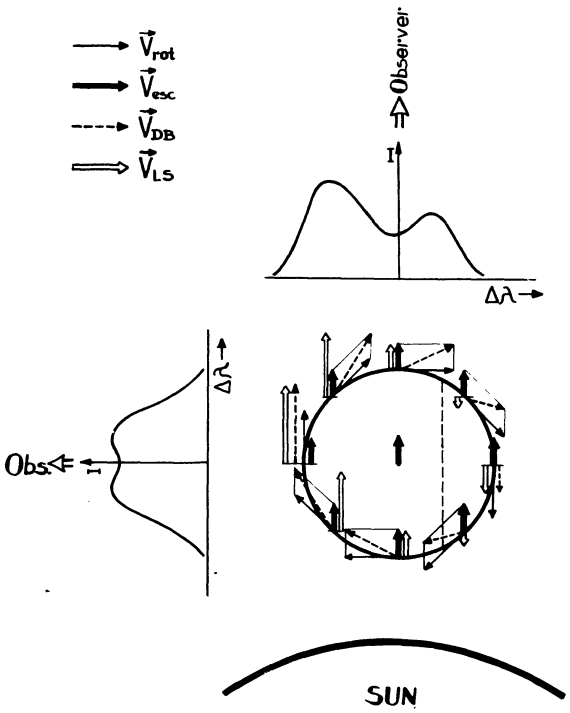

Fig. 1. Schematic picture illustrating the way in which the profiles of the Doppler-brightened lines of a horizontally oriented filament result from the combined action of the rotation and the escape.

In the present paper we would like to show the H_α-profiles for the more interesting case of the disk filaments only. It must be stressed here, however, that contrary to the profiles of the limb filaments, the profiles of the disk filaments are not to be directly compared with the observational profiles. This is so, because the discussed profiles were computed without taking into account the effect of the photospheric radiation coming from behind the filament. A great part of this radiation directly traverses the optically thin filament. Only a small fraction of the radiation is absorbed by the filament and subsequently scattered in all directions. As a result, the brightness of the filament and the solar area, covered by it, becomes less intense than the brightness of the surrounding photosphere. Thus, the profiles, which are considered in this paper, are only the result of the scattering of the incident radiation, emitted by the entire Sun's area visible from the height of the filament. Nevertheless, it is to be noted here that as a result of the Doppler-brightening effect, it is possible to see some optically thin filaments, moving with respect to the Sun, in the emission against the disk. This problem will be treated separately in a forthcoming paper.

The H_α-profiles of the rotating and, at the same time, escaping filaments were computed by means of an ODRA-1204 computer. The following expression has been numerically integrated

$$I_\lambda^D = 2\int_{-R}^{+R} dx \int_0^{\sqrt{R^2-x^2}} \left\{ e^{-\frac{1}{\Delta\lambda_D^2}\left[\Delta\lambda - \frac{\lambda_0}{C}(\omega x + v_0)\right]^2} \cdot A\left(\sqrt{v_0^2 + 2v_0\omega x + \omega^2(x^2+y^2)}\, \frac{v_0 + \omega x}{\sqrt{v_0^2 + 2v_0\omega x + \omega^2(x^2+y^2)}}\right)\right\} dy$$

$$- 2\int_{-r}^{+r} dx \int_0^{\sqrt{r^2-x^2}} \left\{ e^{-\frac{1}{\Delta\lambda_D^2}\left[\Delta\lambda - \frac{\lambda_0}{C}(\omega x + v_0)\right]^2} \cdot A\left(\sqrt{v_0^2 + 2v_0\omega x + \omega^2(x^2+y^2)}\, \frac{v_0 + \omega x}{\sqrt{v_0^2 + 2v_0\omega x + \omega^2(x^2+y^2)}}\right)\right\} dy, \qquad (1)$$

where ω is the angular velocity of rotation, v_0 is the velicity of the escape, denoted by V_{esc} in the diagrams, R the exterior radius of a cylindrical filament or a cylindrical shell, and r the inner radius of a cylindrical shell.

The physical foundations and the way of deriving of Eq. (1) have been shown in Paper I.

The problem to be solved has been formulated in the rectangular system of coordinates x and y, with the observer placed in the direction of the y-axis. Equation (1) enables one to calculate the profiles of the filaments which have the form of cylinders and cylindrical shells. For the cylindrical filaments the second integral term becomes zero. The function A is a dimensionless equivalent of the source function (see Paper I).

The computed profiles are shown in Figs 2 and 3 for several values of the velocity of escape

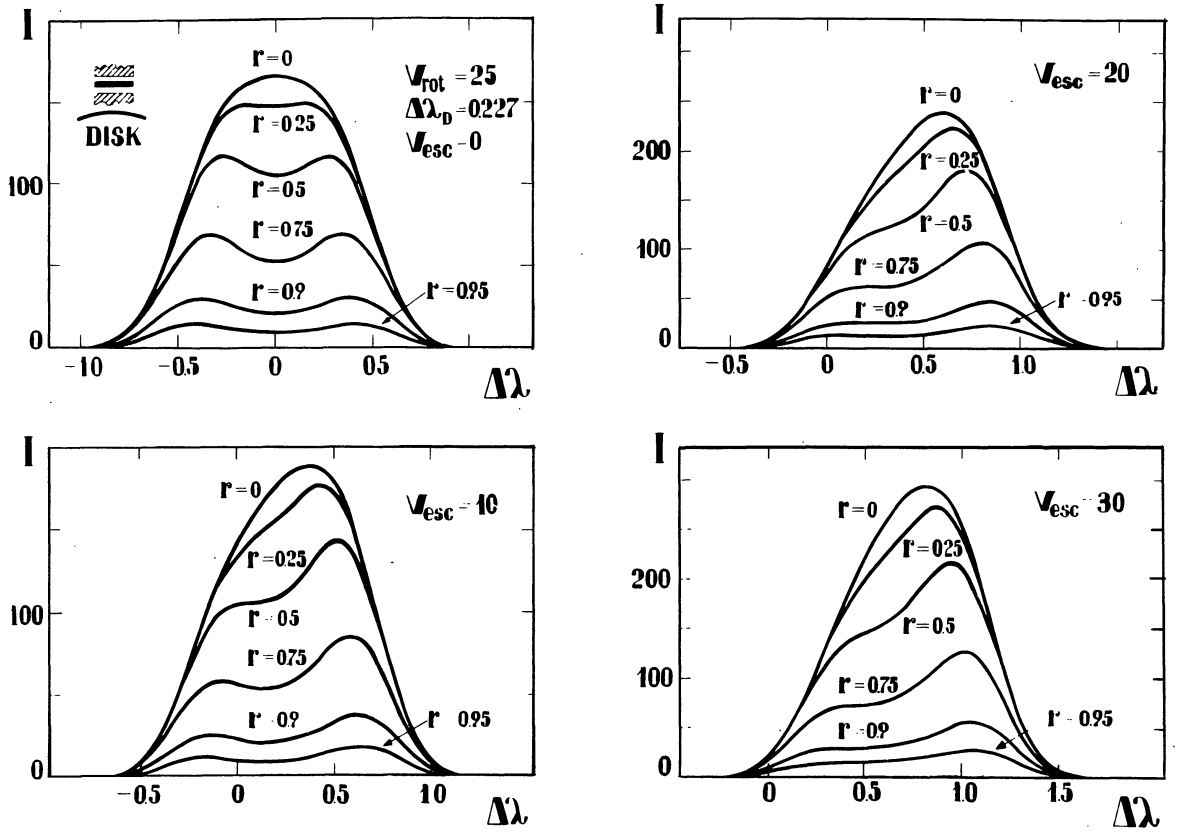

Fig. 2. The H_α Doppler-brightened profiles resulting from the combined action of the rotation and the escape for a peripheral rotational velocity of 25 km s^{-1}.

($V_{esc}=0$, 10, 20 and 30 km s^{-1}), and for various geometries of the filament ($r=0$ – cylinder, $0<r<1$ – cylindrical shells). The peripheral rotational velocity was accepted as 25 km s^{-1} and 100 km s^{-1} for the profiles, presented in Figs 2 and 3, respectively.

The H_α-line profiles due to the pure rotation ($V_{esc}=0$) are symmetric with respect to the line centre, and generally are double-peaked. Only the profile of a slowly rotating cylindrical filament is single-peaked.

The profiles due to the rotation and the escape are asymmetric with respect to the line centre, an exhibit two peaks of unequal intensity in most instances. The asymmetry in the wavelength extension of both the wings, as well as in the maximum intensity of the peaks, becomes larger as the velocity of the escape increases.

3. The Expansion

It is generally known to the Sun's observers that the sizes of some of the fine solar structures (filaments, knots) grow in time, as a result of their radial expansion. In this section we would like to demonstrate the Doppler-brightening effect in the expanding filaments. Unfortunately, we know nothing about the internal structure and about the radial distribution of the velocity in the expanding filaments. Therefore, the H_α-profiles of the expanding filaments, which will be shown here, were constructed for filaments of different geometries and for several radial distributions of the velocity. The accepted form of the radial distributions of the velocity is the following:

$$\begin{aligned} &\text{a)}\ v(d) = -v\,d + V\,, \\ &\text{b)}\ v(d) = \quad V\,d\,, \\ &\text{c)}\ v(d) = \quad V\,, \end{aligned} \tag{2}$$

where $V>0$, and the current radial variable d satisfies the condition $r \leq d \leq R = 1$.

The H_α-profiles of the expanding disk filaments, horizontally oriented to the Sun's surface, were computed from the formula

$$I_\lambda^D = 2 \int_{-R}^{+R} \mathrm{d}x \int_0^{\sqrt{r^2-x^2}} \left\{ \mathrm{e}^{-\frac{1}{\Delta\lambda_D^2}\left[\Delta\lambda - \frac{\lambda_0'}{c}\cdot\frac{y}{\sqrt{x^2+y^2}}\,v\,(\sqrt{x^2+y^2})\right]^2} \right.$$

$$\cdot A\left(v\sqrt{x^2+y^2}, \frac{y}{\sqrt{x^2+y^2}}\right)\Big\}\,dy - 2\int_{-r}^{+r} dx \int_{0}^{\sqrt{r^2-x^2}} \Big\{e^{\frac{1}{\Delta\lambda_D^2}\left[\Delta\lambda - \frac{\lambda_0}{c}\cdot\frac{y}{\sqrt{x^2+y^2}}\cdot v(\sqrt{x^2+y^2})\right]^2} \cdot$$

$$\cdot A\left(v\sqrt{x^2+y^2}, \frac{y}{\sqrt{x^2+y^2}}\right)\Big\}\,dy.$$

the velocity of expansion for the velocity distributions b) and c). For the latter case this increase is especially pronounced. It is evident that simultaneously with the increase of the velocity of expansion the profiles become broader.

In Figure 5 the profiles for filaments of different geometries are compared at a fixed velocity of

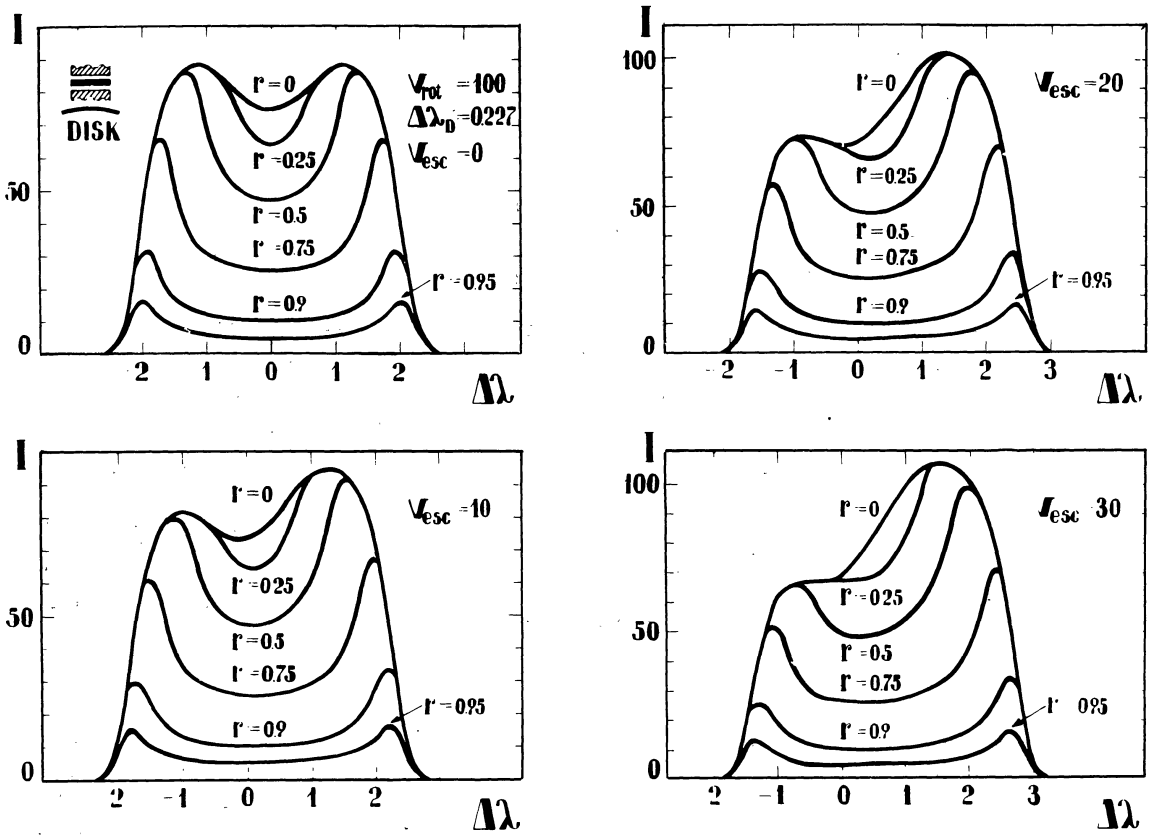

Fig. 3. The H_α Doppler-brightened profiles resulting from the combined action of the rotation and the escape for a peripheral rotational velocity of 100 km s^{-1}.

where $x^2+y^2=d$. The other quantities are the same as in Eq. (1).

The profiles resulting from an expanding cylindrical filament ($r=0$) and the velocity distributions (2) a), b) and c) are presented in Figs. 4a, 4b and 4c, respectively. In every diagram of Figure 4 the profiles for several maximum values of the expansion velocity are compared. The velocity distribution is schematically indicated in the upper right-hand corner of every diagram. The mean intensities of all the profiles shown in Figures 4 and 5 are normalized to 100. The profiles for the velocity distribution a) are single-peaked, while the profiles for the velocity distributions b) and c) are double-peaked. The ratio of the peak intensity to the mean intensity of a profile increases with the increase of expansion (50 km s^{-1}). The shape of the profiles, computed for the velocity distribution a), strongly depends on the thickness of the cylindrical shell filament. The thinner the cylindrical shell, the narrower the profile. For the velocity distribution b) the ratio of the peak intensity to the mean intensity of the profiles is very sensitive to the geometry of the filament. The profiles due to constant distribution of velocity (Fig. 5c) exhibit the same shape independently of the geometrical structure of the filament.

In order to demonstrate clearly the difference between the profiles received from the different distributions of the velocity of expansion, the profiles for all the considered velocity distributions were brought together in every diagram of Figures

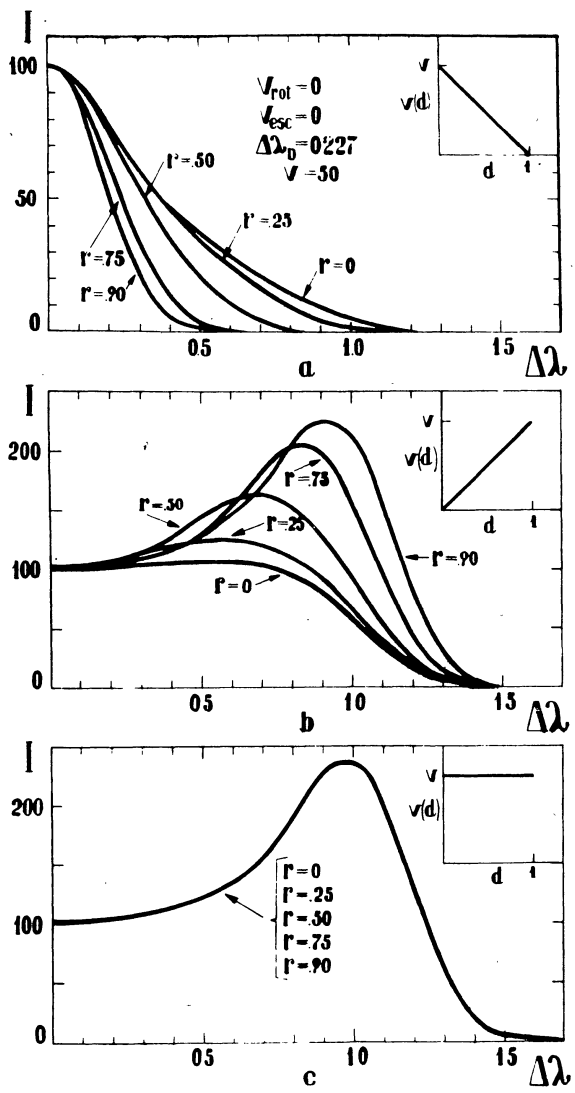

Fig. 4. The H_α Doppler-brightened profiles resulting from an expanding filament for three types of radial velocity distributions (2), and for the maximum value of the velocity of expansion as a parameter.

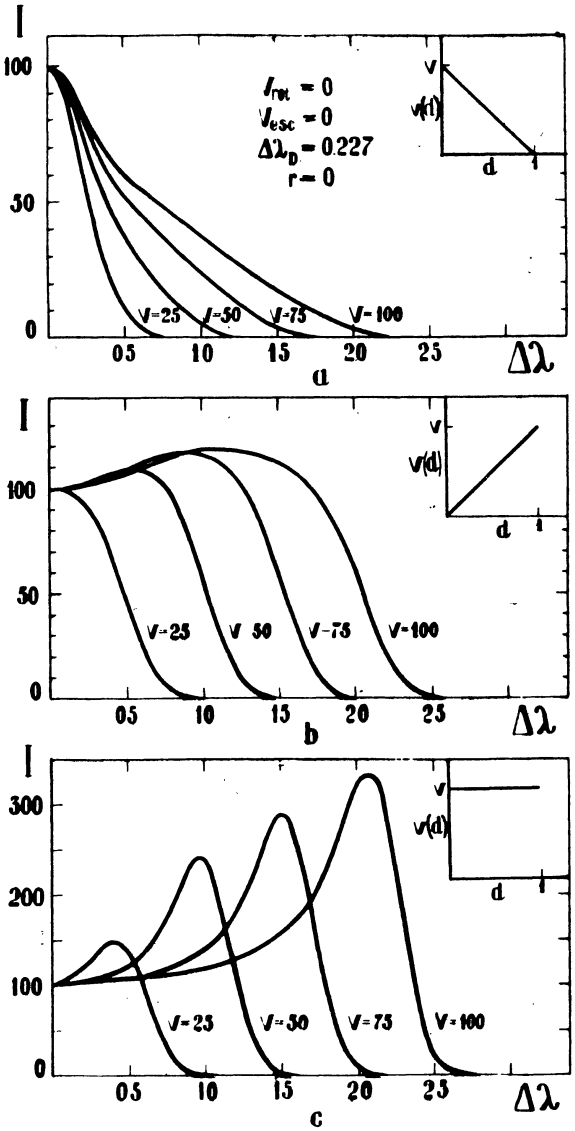

Fig. 5. The H_α Doppler-brightened profiles resulting from an expanding filament for three types of radial velocity distributions (2), and for several different shapes of the filament.

6 and 7. The profiles, presented in Fig. 6, are due to a cylindrical filament ($r=0$), and the profiles, presented in Figure 7, are due to a cylindrical shell ($r=0.75$). Every diagram in Figs 6 and 7 is for a different value of the maximum velocity of expansion. Note, that the profiles for the cylindrical filament and for the assumed velocity distributions (Fig. 6) differ essentially from one another. On the other hand, the profiles for the cylindrical shell and for velocity distributions b) and c) are of very similar shape (Fig. 7).

All the profiles, presented in this section, which are due to expansion, are symmetric with respect to the line centre. It is easily to imagine, by analogy to the profiles discussed in the previous section, that the profiles which could be produced by the combined effect of the expansion and the escape, ought to be asymmetric both in the wavelength extension of the wings and in the maximum intensity of the peaks. The way in which the profiles of the Doppler-brightened lines result from the expanding and the escaping filaments is schematically shown in Figure 8. It is interesting to notice that in the case of a disk filament the broken line dividing the unequal volumes of the filament, participating in formation of the blue and the red part of a line, is horizontally oriented to the Sun. In the case of the combined effect of the rotation and the escape, this

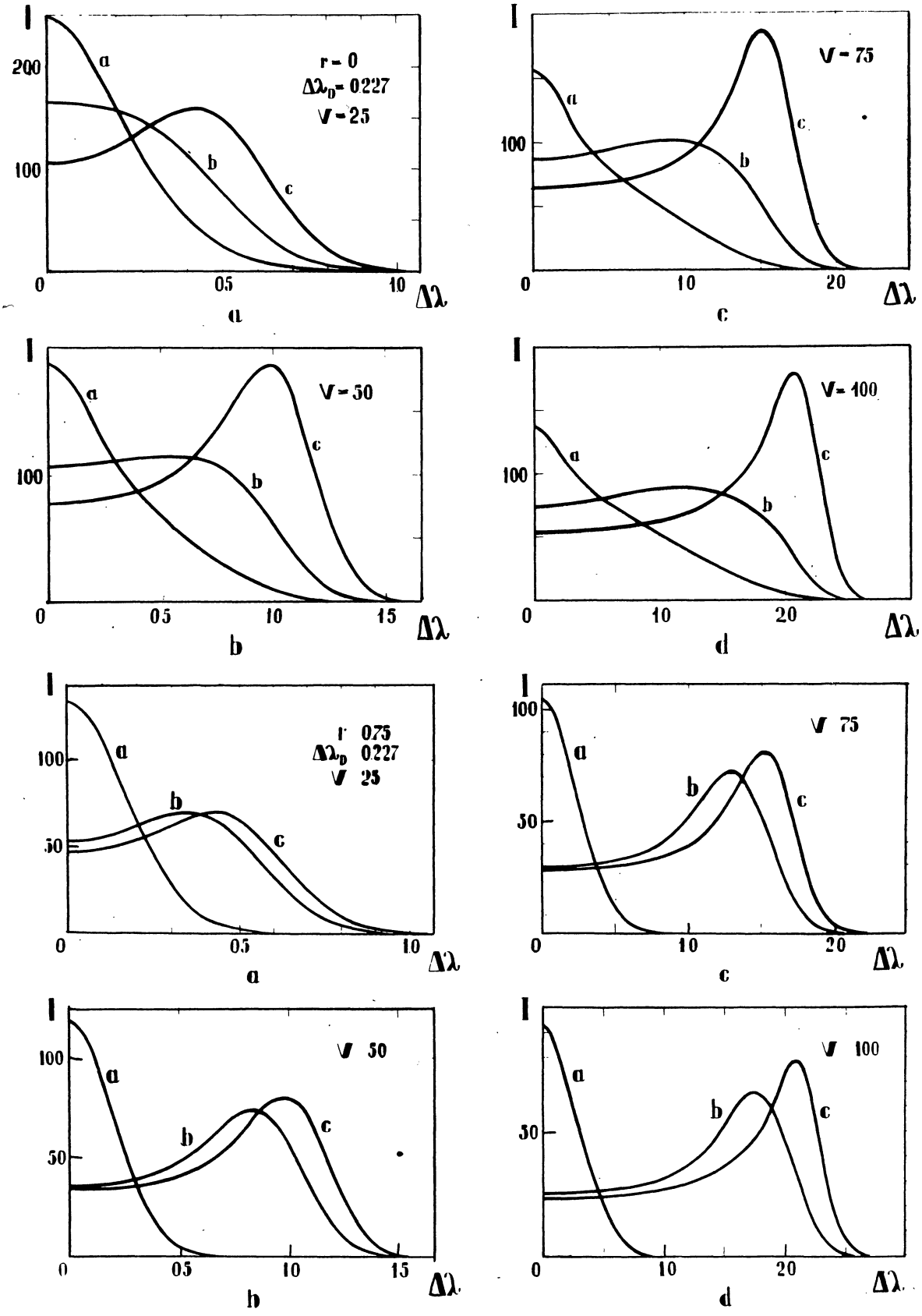

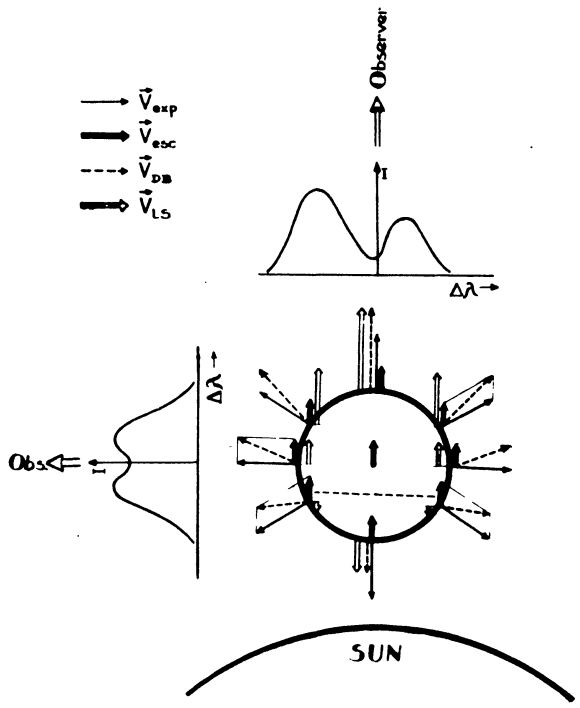

Fig. 8. Schematic picture illustrating the way in which the profiles of the Doppler-brightened lines of a horizontally oriented filament result from the combined action of the expansion and the escape.

broken line was vertically oriented to the Sun (cf. Fig. 1).

The Doppler-brightened H_α-profiles, resulting from the combined action of the expansion and the escape, will be treated in a forthcoming paper.

4. Final Remarks

Although the Doppler-brightened profiles, presented in Sections 2 and 3, were computed for the H_α-line, one may expect generally similar effects in the profiles of the other lines, formed by the scattering the Sun's incident radiation, provided that every line possesses a well-marked absorption line in the photospheric spectrum.

The analysis of the profiles, performed in the present paper, as well as in Paper I, shows that as a result of the Doppler-brightening effect it is possible to get a wealth of substantially different line profiles from some fine active solar structures. This is especially the case for the structures in which the line-broadening effects, caused by macroscopic motions, prevail over the effects of other line broadening mechanisms. Therefore, one must be extremely careful in applying the traditional spectral analysis procedure for deriving some physical parameters of the investigated plasma.

References

ROMPOLT, B. (1971): Publ. Heliophysical Observ. Debrecen (in press).

ROMPOLT, B. (1974): Acta Universitatis Wratislaviensis (in press).

ROMPOLT, B. (1976): In this volume.

◀ Fig. 6. The H_α Doppler-brightened profiles resulting from an expanding cylindrical filament ($r = 0$) for velocity distributions (2) a), b) and c).

◀ Fig. 7. The H_α Doppler-brightened profiles resulting from an expanding cylindrical shell ($r = 0.75$) for velocity distributions (2) a), b) and c).